

Actin Glutathionylation Increases in Fibroblasts of Patients with Friedreich's Ataxia

A POTENTIAL ROLE IN THE PATHOGENESIS OF THE DISEASE*

Received for publication, February 21, 2003, and in revised form, August 8, 2003
Published, JBC Papers in Press, August 11, 2003, DOI 10.1074/jbc.M301872200

Anna Pastore‡, Giulia Tozzi§, Laura Maria Gaeta§, Enrico Bertini§, Valentina Serafini‡,
Silvia Di Cesare¶, Valentina Bonetto¶**, Filippo Casoni¶, Rosalba Carrozzo§, Giorgio Federici‡,
and Fiorella Piemonte§‡‡

From the ‡Laboratory of Biochemistry and the §Molecular Medicine and ¶Flow Cytometric Units, Children's Hospital and Research Institute "Bambino Gesù," Piazza S. Onofrio, 4, 00165 Rome, Italy and the ¶Dulbecco Telethon Institute, Pharmacological Research Institute "Mario Negri," Via Eritrea, 62, 20157 Rome, Italy

Increasing evidence suggests that iron-mediated oxidative stress might underlie the development of neurodegeneration in Friedreich's ataxia (FRDA), an autosomal recessive ataxia caused by decreased expression of frataxin, a protein implicated in iron metabolism. In this study, we demonstrate that, in fibroblasts of patients with FRDA, the cellular redox equilibrium is shifted toward more protein-bound glutathione. Furthermore, we found that actin is glutathionylated, probably as a result of the accumulation of reactive oxygen species, generated by iron overload in the disease. Indeed, high-pressure liquid chromatography analysis of control fibroblasts *in vivo* treated with FeSO₄ showed a significant increase in the protein-bound/free GSH ratio, and Western blot analysis indicated a relevant rise in glutathionylation. Actin glutathionylation contributes to impaired microfilament organization in FRDA fibroblasts. Rhodamine phalloidin staining revealed a disarray of actin filaments and a reduced signal of F-actin fluorescence. The same hematoxylin/eosin-stained cells showed abnormalities in size and shape. When we treated FRDA fibroblasts with reduced glutathione, we obtained a complete rescue of cytoskeletal abnormalities and cell viability. Thus, we conclude that oxidative stress may induce actin glutathionylation and impairment of cytoskeletal functions in FRDA fibroblasts.

Oxidative stress has been proposed to underlie neurodegeneration in Friedreich's ataxia (FRDA),¹ the most common of the hereditary ataxias, caused by severely reduced levels of frataxin, a protein implicated in iron metabolism. FRDA is characterized by degeneration of the large sensory neurons and spinocerebellar tracts, cardiomyopathy, and increased incidence of diabetes. Most patients (95%) are homozygous for the hyperexpansion of a GAA repeat sequence in the first intron of the frataxin gene; a few are heterozygous for a GAA expansion

* This work was supported in part by Grant R-03-30 from the "Fondazione Pierfranco e Luisa Mariani," Italy. The costs of publication of this article were defrayed in part by the payment of page charges. This article must therefore be hereby marked "advertisement" in accordance with 18 U.S.C. Section 1734 solely to indicate this fact.

** Assistant Telethon Scientist supported by Grant TCP.01010 from Telethon, Italy.

‡‡ To whom correspondence should be addressed. Tel.: 390-6-6859-2105; Fax: 390-6-6859-2024; E-mail: piemonte@opbg.net.

¹ The abbreviations used are: FRDA, Friedreich's ataxia; HPLC, high-pressure liquid chromatography; EE-GSH, ethyl ester-reduced glutathione.

and a point mutation (1–3). Data from yeast suggest that frataxin deficiency results in iron accumulation within mitochondria and increased sensitivity to oxidative stress (4, 5). Mouse models for FRDA exhibit cardiomyopathy, sensory nerve defects, and Fe-S enzyme deficiency followed by intramitochondrial iron deposits (6). Patients with FRDA have iron deposits in the heart, increased mitochondrial iron in fibroblasts, and greater sensitivity to oxidative stress by pro-oxidants such as FeCl₃ and hydrogen peroxide (3, 7, 8). Furthermore, a defective mitochondrial respiratory chain has been found in FRDA tissues, in association with iron accumulation and moderate decreases in mtDNA levels (9, 10).

Iron is a crucial reagent in the Fenton reaction, as it can react with mitochondrially generated superoxide anion (O₂⁻) to produce the toxic hydroxyl radical (OH[•]), and iron-mediated oxidative stress has been hypothesized to underlie the pathophysiology of the disease. Increased levels of oxidative stress markers such as plasma malondialdehyde and urine 8-hydroxy-2-deoxyguanosine have been found in patients with FRDA, and improvement of cardiac and skeletal muscle bioenergetics has been observed after antioxidant treatment (11–15). Moreover, we found an impairment *in vivo* of the antioxidant enzymes superoxide dismutase and glutathione peroxidase and decreased levels of free glutathione in the blood of patients with FRDA (16, 17).

In cells, exposure to acute oxidative stress triggers a sequence of events characterized by depletion of antioxidant defenses and oxidative modification of proteins, lipids, and nucleic acids. Protein thiols are particularly susceptible to oxidation and may represent important targets in redox signaling. Recently, protein glutathionylation has gained attention as a possible means of protein function redox regulation. One proposed mechanism leading to protein *S*-glutathionylation *in vivo* is the thiol/disulfide exchange mechanism (18), which occurs when an oxidative insult changes the GSH/GSSG ratio and induces GSSG to bind to protein thiols. Several important enzymes, including phosphofructokinase (19), glycogen synthase (20), fructose-1,6-diphosphatase (21), 3-hydroxy-3-methylglutaryl-CoA reductase (22), glyceraldehyde-3-phosphate dehydrogenase (23), protein kinase C (24), and guanylate cyclase (25), and glucocorticoid receptors (26) are potentially influenced by the formation of protein adducts with glutathione. Also transcription factors such as c-Jun appear to be redox-regulated by mechanisms that include protein *S*-thiolation (27, 28), and ubiquitin-activating enzymes become *S*-glutathionylated, with a concomitant decrease in the ubiquitinylation pathway, when cells are exposed to oxidants (29). A reversible

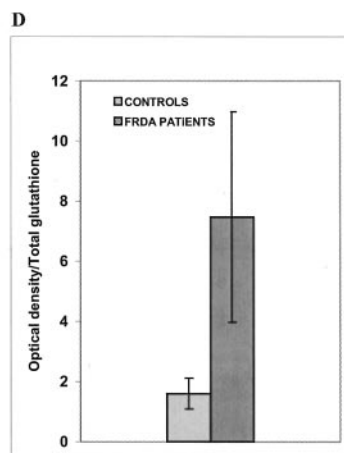
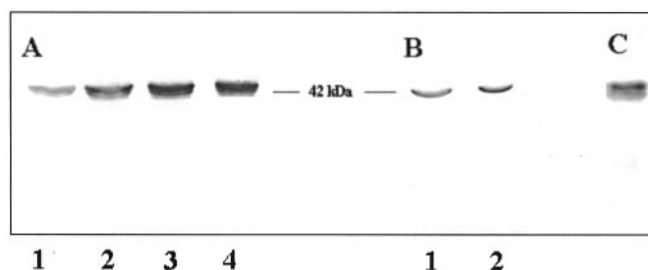
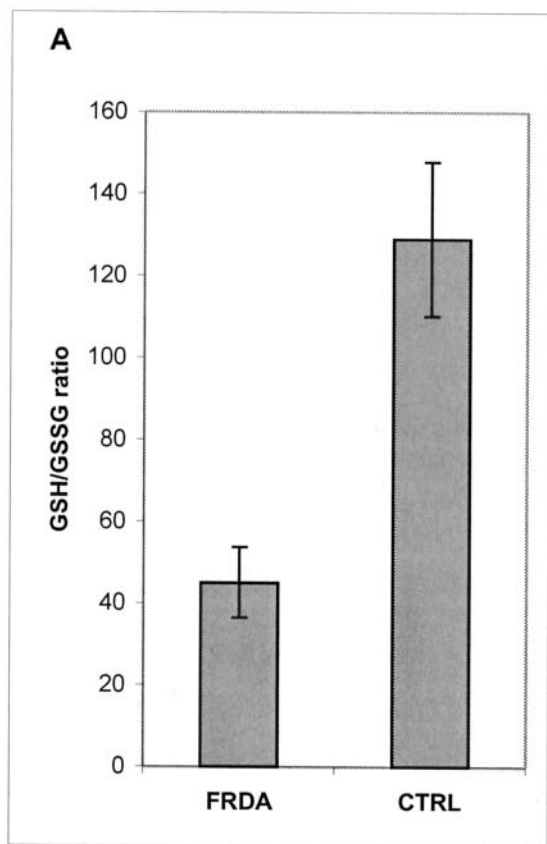


FIG. 2. Glutathionylated proteins in fibroblasts of FRDA patients. A, glutathione bound to proteins was immunologically detected by Western blot analysis. Equal amounts of fibroblast lysates (40 μ g) were separated by SDS-PAGE and transferred to nitrocellulose. The glutathione conjugates were probed with monoclonal anti-GSH antibody. Lane 1, control; lanes 2-4, FRDA fibroblasts obtained from three exemplifying patients. B, fibroblast lysates were analyzed by Western blotting using anti-actin antibody. Lane 1, control; lane 2, FRDA fibroblasts (corresponding to the sample in lane 2 of A). C, anti-GSH antibody was used for immunochemical detection of immunoprecipitated actin from FRDA fibroblasts. D, nitrocellulose filters were subjected to densitometric analysis and normalized by calculating the ratios between mean optical density of FRDA patients ($n = 9$) or controls ($n = 4$) and total glutathione concentrations as obtained by HPLC analysis.

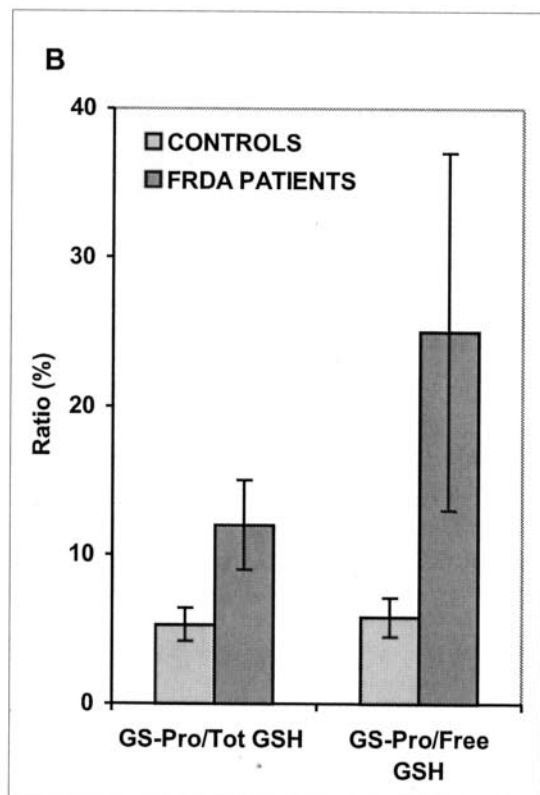


FIG. 1. HPLC analysis of glutathione status in FRDA fibroblasts. The GSH/GSSG ratios (A) and protein-bound (GS-Pro)/total (Tot) GSH and protein-bound/free GSH ratios (B) were determined in FRDA fibroblasts ($n = 9$) and in controls (CTRL; $n = 4$). For all experiments, $p < 0.05$. For details, see "Experimental Procedures."

glutathionylation was found to regulate actin polymerization in human epidermal carcinoma cells (30), and S-glutathionylation, followed by inactivation, was reported for creatine kinase, a crucial source of ATP in myocytes, during oxidative stress (31). Furthermore, we recently found an increase in glutathionyl-hemoglobin in the blood of patients with FRDA, accompanied by a significant decrease in free glutathione (17).

Free glutathione concentration, mainly represented by its reduced form, is a limiting factor in many detoxifying processes by protecting protein thiol groups from oxidation, directly as a free radical scavenger or as a cosubstrate for a number of important enzymes such as glutathione peroxidase and glutathione transferases (32). Under conditions of increased oxidant stress such as ischemia/reperfusion, chronic ethanol ingestion, tumor necrosis factor-induced cytotoxicity, and bile acid retention in cholestasis, glutathione status is a critical factor in determining loss of mitochondrial function and cell viability as well as transcription factor activation and gene regulation (33). The relation existing among glutathione, oxidative stress, and neurodegeneration was recently reviewed by Schulz *et al.* (34), and an important role for glutathione has been proposed for the pathogenesis of Parkinson's disease, where a decrease in GSH concentrations in the substantia nigra was observed in preclin-

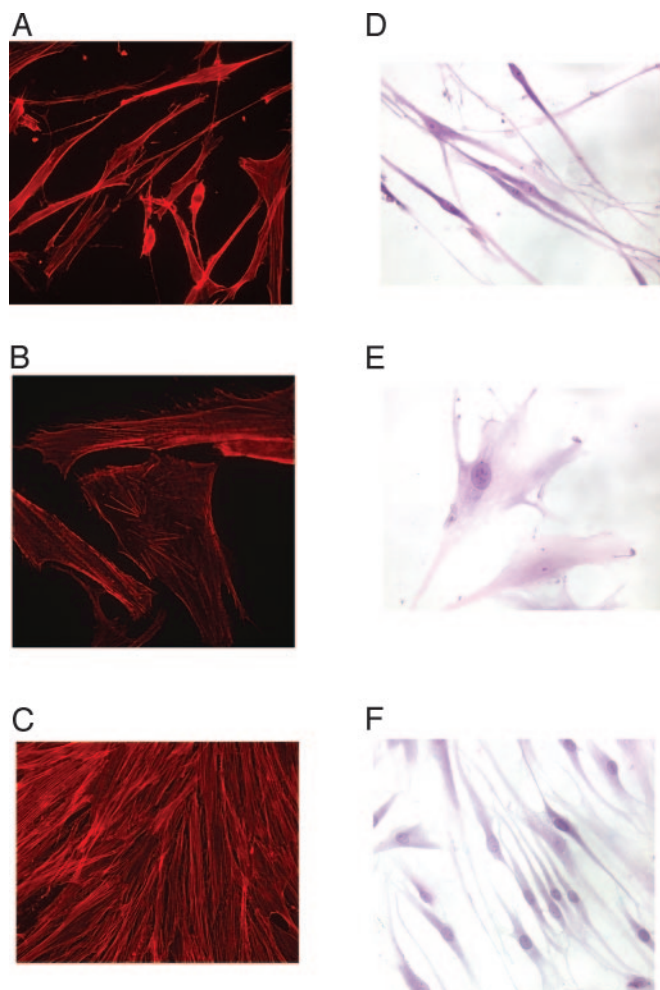


FIG. 3. Fluorescence and light microscopy images of fibroblasts at the same magnification ($\times 40$). Actin was visualized by rhodamine phalloidin staining. Clear fluorescence attenuation appeared in fibroblasts of FRDA patients (B), together with enlargement of the cytoplasmic area and disarray of actin filaments, compared with control cells (A). The same FRDA cells stained with hematoxylin and eosin showed marked enlargement of cell size as well as abnormal shape (E) with respect to control cells (D). Rescue of fluorescence intensity (C) and of cytoskeletal abnormalities (F) in FRDA cells was obtained after incubation for 30 days at 37 °C with 10 mM GSH.

ical stages of the disease (35). Although the pathogenesis of FRDA is still unclear, one possibility is that the presence of unbound (free) reactive iron, via the Fenton reaction, generates free radicals within the mitochondria, leading to oxidative damage.

Thus, in light of accumulating evidence indicating a crucial role for glutathione in the regulation of cellular signaling in response to oxidative and nitrosative stress (36, 37), we analyzed the redox status of glutathione in fibroblasts of patients with FRDA and identified a protein that undergoes glutathionylation in these patients. For this purpose, we cultured skin biopsies obtained from nine patients with FRDA and determined total, free, reduced, oxidized, and protein-bound glutathione concentrations by high-pressure liquid chromatography (HPLC) analysis. In addition, we analyzed the glutathionylated protein pattern by Western blotting using a monoclonal anti-GSH antibody.

EXPERIMENTAL PROCEDURES

Materials—Monoclonal anti-GSH antibody was obtained from Virogen. Polyclonal anti-actin antibody and 6-carboxyfluorescein (apoptosis detection kit) were from Sigma. Rhodamine phalloidin was from Molecular Probes, Inc. Protein G PLUS-agarose was from Santa Cruz Bio-

technology. The BCA protein assay was obtained from Pierce. All materials for cell cultures were from Invitrogen; all other chemicals were from Sigma.

Cell Culture—Skin biopsies were taken from nine clinically affected (and genetically proven) FRDA patients (four males and five females) and four age-matched controls. Fibroblasts were grown in Dulbecco's modified Eagle's medium supplemented with 10% fetal bovine serum, 50 units/ml penicillin, 50 μ g/ml streptomycin, 0.4% (v/v) amphotericin B (250 μ g/ml), and 1 mM sodium pyruvate at 37 °C in 5% CO₂. Fibroblasts were grown to 90% confluence. The assays were performed in triplicate, and each fibroblast strain was separately grown and processed twice. Cells were used at similar passage numbers. After washing with phosphate-buffered saline, the cells were resuspended in 100 μ l of H₂O, sonicated three times for 2 s (Sonics Vibra Cell, Sonics & Material Inc., Newtown, CT), and subjected to biochemical analysis.

HPLC Determination of Various Forms of Glutathione—The cells (treated differently) were sonicated three times for 2 s in 0.1 ml of 0.1 M potassium phosphate buffer (pH 7.2). After sonication, 50 μ l of 12% sulfosalicylic acid were added, and the GSH content in the acid-soluble fraction was determined (free GSH). The protein pellet was dissolved in 150 μ l of 0.1 N NaOH, and protein-bound GSH was determined. To measure oxidized glutathione (GSSG), cells were sonicated three times for 2 s in 0.1 ml of 0.1 M potassium phosphate buffer (pH 7.2) containing 10 mM *N*-ethylmaleimide. Total GSH was determined in fibroblast lysates before adding 12% sulfosalicylic acid. GSH levels were calculated by subtracting GSSG concentrations from free GSH values. Protein concentrations were quantified by the BCA protein assay. Derivatization and chromatography procedures were carried out as previously reported (38).

Analysis of Glutathione Conjugates by Western Blotting—40 μ g of lysate sample were subjected to 12% SDS-polyacrylamide gel electrophoresis, and the proteins were transferred to a nitrocellulose membrane overnight at 70 mA. The membrane was blocked with 5% nonfat dry milk in 100 mM NaCl and 10 mM Tris-HCl (pH 7.8) containing 0.1% Tween 20 for 2 h at room temperature and probed with monoclonal anti-GSH antibody (1:500) and/or polyclonal anti-actin antibody (1:1000).

Identification of Glutathionylated Actin by Immunoprecipitation—Fibroblasts (resuspended in 150 μ l of H₂O and sonicated) were incubated with 50 μ l of anti-actin antibody (1 μ g) for 1 h at 4 °C, and 50 μ l of the resuspended volume of protein G PLUS-agarose were added to the solution and incubated at 4 °C for 1 h on a rocker platform. The pellet was collected by centrifugation at 800 \times *g* for 5 min at 4 °C and washed four times with phosphate-buffered saline. After a final wash, the pellet was resuspended in 10 μ l of electrophoresis sample buffer, boiled for 2 min, loaded onto a nonreducing 12% SDS-polyacrylamide gel for Western blot analysis, and revealed with anti-GSH antibody (1:500).

Quantification of Glutathionylated Actin—The extent of glutathionylation was quantified by analyzing nitrocellulose filters with a Bio-Rad Model GS-670 imaging densitometer. Data were analyzed using Bio-Rad Molecular Analyst™ software (Version 1.3) and normalized to the quantity of protein loaded on the gels and to total glutathione content in fibroblasts.

Fluorescence Microscopy Analysis of Rhodamine Phalloidin-stained Fibroblasts—Cells were washed twice with phosphate-buffered saline, fixed in 3.7% formaldehyde solution for 10 min at room temperature, permeabilized with 0.1% Triton X-100, and stained with rhodamine phalloidin. Fluorescent images were monitored using a Zeiss microscope (Axioskobe 50) equipped with epifluorescence and a $\times 40$ objective.

Cell Morphology—Cells grown on Falcon chamber slides (BD Biosciences) were washed twice with phosphate-buffered saline, fixed in 3.7% formaldehyde solution for 10 min, and stained with Harris hematoxylin for 7 min. After treatment with 0.1% (v/v) HCl, cells were washed with H₂O for 10 min, stained with eosin for 20 s, dried with ethanol (70, 95, and 100%, v/v), and washed with xylol. Images were monitored using the Axioskobe 50 microscope equipped with a $\times 40$ objective.

Effect in Vivo of GSH, Ethyl Ester-reduced Glutathione (EE-GSH), and Acivicin on Actin Glutathionylation and Cell Morphology and Viability—Fibroblasts of three patients with FRDA were incubated for 30 days at 37 °C with 10 mM (final concentration) GSH and 10 mM (final concentration) EE-GSH in both the absence and presence of 150 μ M (final concentration) acivicin, a γ -glutamyltranspeptidase inhibitor. Cell lysates were analyzed by Western blotting as described above to determine the extent of actin glutathionylation. GSH-treated FRDA cells were subjected to fluorescence and light microscopy by staining with rhodamine phalloidin and hematoxylin/eosin, respectively (see

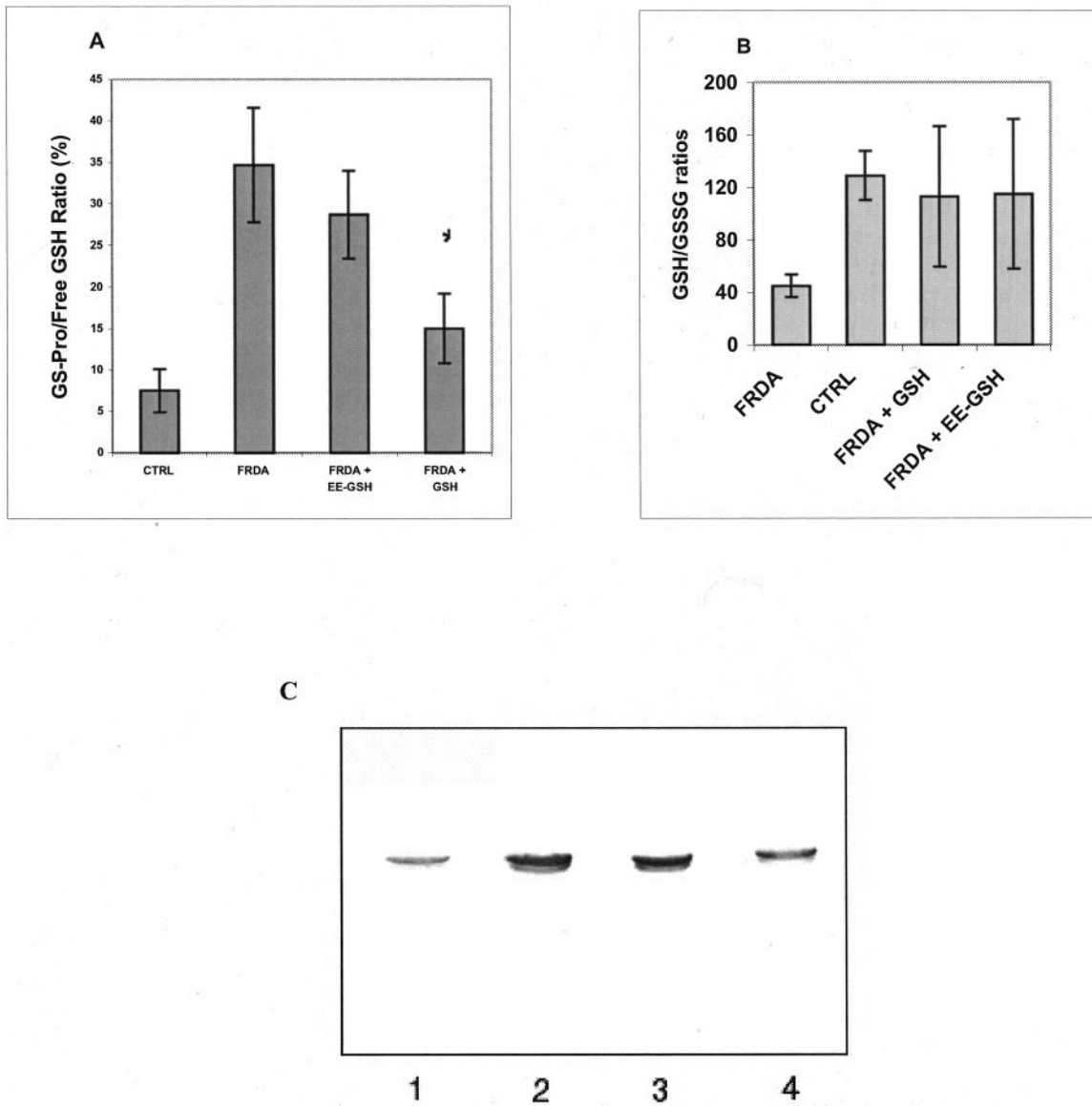


FIG. 4. *In vivo* reversibility of actin glutathionylation by treatment with antioxidant compounds. Fibroblasts obtained from FRDA patients were treated *in vivo* with 10 mM GSH and 10 mM EE-GSH for 30 days at 37 °C. **A**, data obtained by HPLC analysis of the protein-bound (*GS-Pro*)/free GSH ratio ($n = 3$). *, $p < 0.05$. **B**, GSH/GSSG ratios as determined by HPLC analysis in controls (*CTRL*; $n = 4$), in FRDA cells ($n = 9$), and in GSH- and EE-GSH-treated FRDA fibroblasts ($n = 3$; $p < 0.05$ compared with untreated FRDA cells). **C**, Western blot analysis of untreated control fibroblasts (*lane 1*), untreated FRDA fibroblasts (*lane 2*), EE-GSH-treated FRDA cells (*lane 3*), and GSH-treated FRDA fibroblasts (*lane 4*). The blot is representative of one of three independent experiments for each condition tested. For details, see "Experimental Procedures."

above). Cell viability was measured using 6-carboxyfluorescein, a non-fluorescent compound that becomes fluorescent in live cells by the action of esterases. Flow cytometric analyses were performed on a FACSCalibur flow cytometer (BD Biosciences), and the results were analyzed using the CellQuest program (BD Biosciences).

Effect *In Vivo* of $FeSO_4$ Treatment on Actin Glutathionylation—The effect of $FeSO_4$ treatment was studied by incubating control fibroblasts *in vivo* with 100 μM (final concentration) $FeSO_4$ or H_2O at 37 °C for 6, 24, 48, 96, and 192 h. Protein-bound/free GSH levels were determined by HPLC analysis as described above. Western blot analysis was performed on cells treated with 100 μM $FeSO_4$ at 37 °C for 24 and 192 h.

Effect *In Vivo* of $FeSO_4$ Treatment on Cell Morphology—Control fibroblasts were treated *in vivo* with 100 μM (final concentration) $FeSO_4$ for 1 month and subjected to fluorescence microscopy by staining with rhodamine phalloidin (see above).

RESULTS

We analyzed the glutathione content in fibroblasts of nine FRDA patients and determined the GSH/GSSG ratios (Fig. 1A) and protein-bound/total GSH and protein-bound/free GSH ra-

tios (Fig. 1B). The GSH/GSSG ratio was 129 ± 18.8 in controls and decreased to 45 ± 8.6 in FRDA fibroblasts ($p < 0.05$). The protein-bound/total GSH ratio was 0.05 ± 0.01 in control cells and increased to 0.12 ± 0.03 in FRDA cells ($p < 0.05$). The protein-bound/free GSH ratio was 0.056 ± 0.013 in control fibroblasts and increased to 0.25 ± 0.12 in FRDA patients ($p < 0.05$). These results indicate that FRDA fibroblasts undergo oxidative stress, with the cellular redox equilibrium shifted toward more protein-bound glutathione with respect to fibroblasts of healthy subjects.

Monoclonal anti-GSH antibody was used to investigate the glutathionylation state of FRDA fibroblasts (Fig. 2). Western blot analysis of fibroblasts obtained from three patients revealed a 42-kDa band (Fig. 2A), which was also detected by anti-actin antibody (Fig. 2B). To identify the 42-kDa protein, we immunoprecipitated the fibroblast lysates with anti-actin antibody and probed them with anti-GSH antibody. As shown

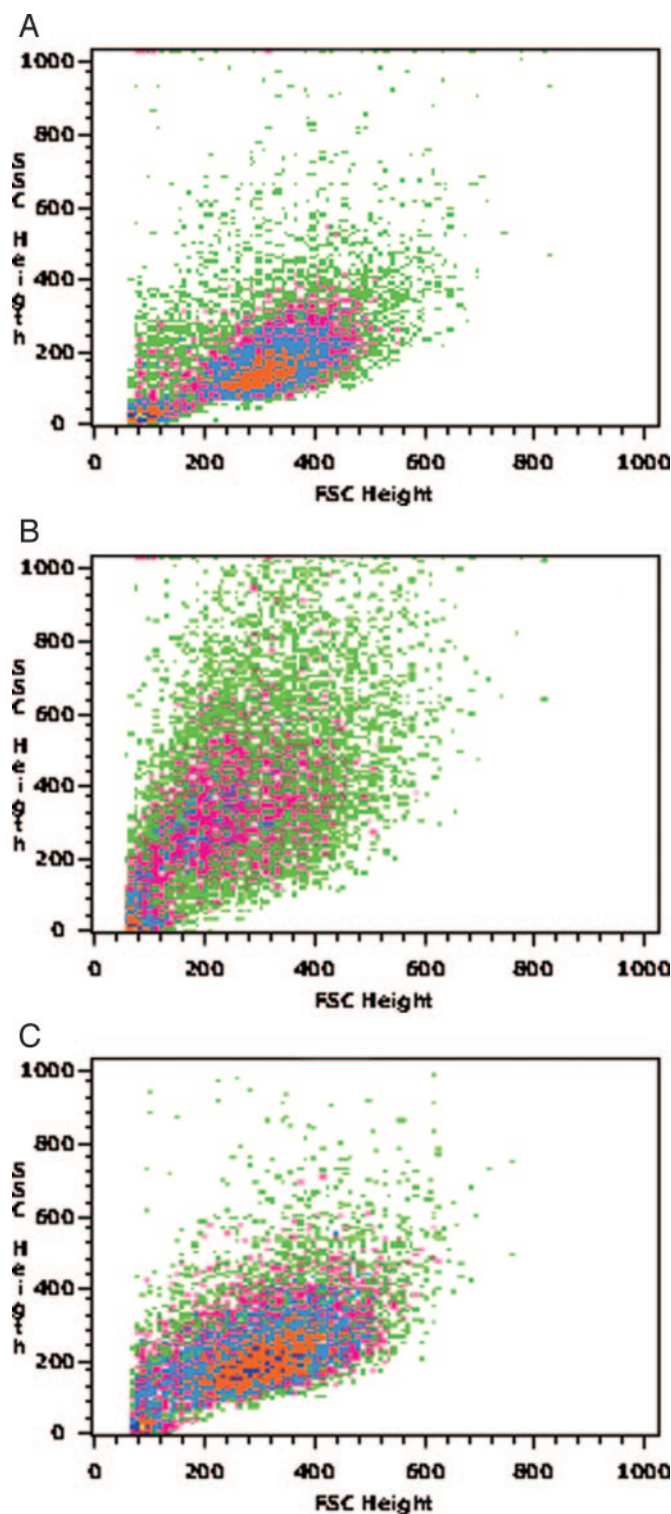


FIG. 5. Cell morphology of fibroblast cell population as assessed by light scattering parameters with density plot of control (A), untreated FRDA (B), and GSH-treated FRDA (C) cells after staining with 6-carboxyfluorescein. Forward scatter (FSC) measures the relative size, whereas side scatter (SSC) is related to the relative granularity or internal complexity.

in Fig. 2C, we obtained a 42-kDa band corresponding to glutathionylated actin. The extent of glutathionylation was increased by 4.7-fold in FRDA patients with respect to controls (7.47 ± 3.5 versus 1.6 ± 0.51 ; $p < 0.05$) (Fig. 2D). Equal amounts of loaded protein SDS were verified by Coomassie Blue staining of an equivalent SDS gel (data not shown).

To investigate whether the unexpected increase in actin glutathionylation in FRDA fibroblasts is related to changes in the cytoskeletal organization, we stained fibroblasts with the filamentous actin indicator rhodamine phalloidin. The fluorescent images revealed a significant disarrangement of F-actin in FRDA patients (Fig. 3B), with clear attenuation of the fluorescent signal compared with controls (Fig. 3A). Under light microscopy, FRDA fibroblasts (Fig. 3E) appeared to be enlarged with respect to fibroblasts of healthy subjects (Fig. 3D). Taken together, these observations suggest that glutathionylation of actin leads to a disarray of actin filaments, inducing size and shape abnormalities in FRDA fibroblasts.

To determine whether there is an *in vivo* reversibility of glutathionylation in FRDA fibroblasts, we treated FRDA cells with 10 mM (final concentration) GSH and 10 mM (final concentration) EE-GSH for 30 days at 37 °C. Fig. 4A illustrates the results from HPLC analysis, showing a $17 \pm 3.7\%$ decrease in the protein-bound/free GSH ratio in EE-GSH-treated FRDA fibroblasts and a $56 \pm 6.8\%$ reduction in GSH-treated FRDA fibroblasts compared with untreated cells. HPLC analysis of GSH and GSSG levels (Fig. 4B) revealed increases in GSH/GSSG ratios to 113 ± 53.5 upon GSH treatment and to 115 ± 57 upon EE-GSH treatment with respect to untreated FRDA cells (45 ± 8.6 ; $p < 0.05$), thus becoming comparable to those in controls (129 ± 18.8). Furthermore, Western blot analysis showed a $20 \pm 5.5\%$ decrease in glutathionylated proteins in EE-GSH-treated cells (Fig. 4C, lane 3) and a $60 \pm 15\%$ decrease in GSH-treated cells (lane 4) compared with untreated FRDA fibroblasts (lane 2). To elucidate how medium GSH is available to the cells, we performed *in vivo* experiments by treating FRDA fibroblasts with acivicin ($150 \mu\text{M}$), an inhibitor of γ -glutamyltranspeptidase. Our findings show that acivicin blocked the protection obtained by GSH treatment, whereas EE-GSH, which is membrane-permeable, was not affected by the inhibitor (data not shown).

The fluorescent images of FRDA fibroblasts after 1 month of *in vivo* GSH treatment showed an increase in the rhodamine phalloidin signal of F-actin (Fig. 3C) and a rescue of cell size and shape (Fig. 3F). Flow cytometric analysis using the cell viability indicator 6-carboxyfluorescein showed a $15.5 \pm 5.6\%$ ($p < 0.05$) increase in the fluorescent signal in GSH-treated FRDA cells (Fig. 5C) with respect to untreated cells (Fig. 5B), comparable to that in controls (Fig. 5A).

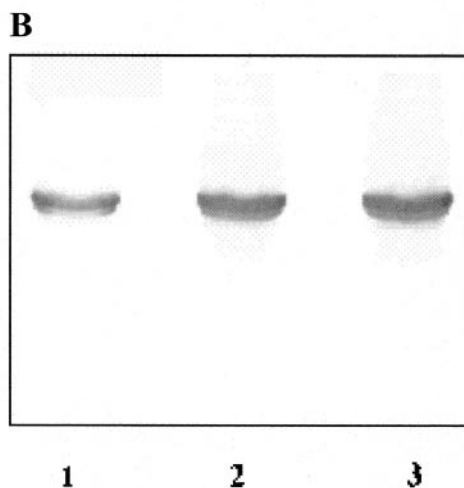
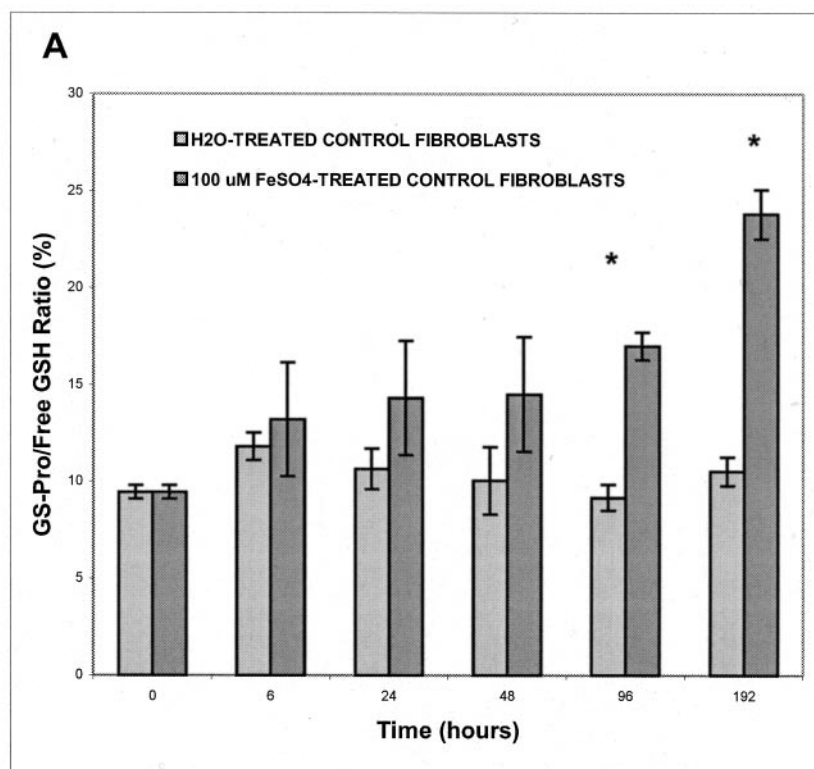
Finally, to determine whether there is an *in vivo* association between iron overload, which underlies the pathogenesis of FRDA, and actin glutathionylation, we treated control fibroblasts with $100 \mu\text{M}$ FeSO_4 for 6, 24, 48, 96, and 192 h. HPLC analysis showed 1.12-, 1.34-, 1.44-, 1.85-, and 2.3-fold increases in the protein-bound/free GSH ratio, respectively, compared with H_2O treatments (Fig. 6A). Western blot analysis of fibroblasts incubated with $100 \mu\text{M}$ FeSO_4 for 24 and 192 h at 37 °C showed 1.7-fold (Fig. 6B, lane 2) and 2-fold (lane 3) increases in glutathionylated actin, respectively, compared with H_2O -treated cells (lane 1). Moreover, to determine whether FeSO_4 induces morphological changes characteristic of FRDA, we treated *in vivo* control cells with FeSO_4 for 1 month without obtaining any significant morphological changes resembling those in FRDA fibroblasts (Fig. 7).

DISCUSSION

The prevailing hypothesis underlying the pathogenesis of FRDA supposes that frataxin is involved in the regulation of mitochondrial iron export and that impaired intramitochondrial iron metabolism results in iron overload and oxidative stress (1, 2). Iron deposits are observed consistently in some heart myofibrils of FRDA patients upon autopsy, and recent magnetic resonance imaging data indicate that iron also accu-

FIG. 6. *In vivo* effect of FeSO_4 treatments on protein glutathionylation.

A, after incubating control cells with H_2O or $100 \mu\text{M}$ FeSO_4 for the indicated times, protein-bound (*GS-Pro*)/free GSH levels were determined by HPLC analysis. Results represent the mean of three independent determinations. B, after treatment with FeSO_4 , control fibroblasts were analyzed by Western blotting. Control cells were incubated at 37°C for 192 h with H_2O (lane 1) or with $100 \mu\text{M}$ FeSO_4 for 24 h (lane 2) and 192 h (lane 3). The blot is representative of one of at least three identical experiments for each condition tested. For details, see "Experimental Procedures."



mulates in the dentate nucleus (9, 39, 40). In previous studies, we reported a significant increase in glutathionyl-hemoglobin in the blood of patients with FRDA, together with an imbalance between the superoxide dismutase and glutathione peroxidase antioxidant enzyme activities, thus supporting the presence of a systemic oxidative stress in the disease (16, 17). Therefore, in light of these recent advances in the pathogenesis of FRDA, our study has focused on the analysis of glutathione metabolism in fibroblasts of FRDA patients. Furthermore, as the oxidized and reduced glutathione redox ratios affect the state of glutathionylated proteins, we also studied the glutathionylated protein pattern in FRDA fibroblasts.

Our findings show, for the first time, that fibroblasts of patients with FRDA undergo oxidative stress, with a significant decrease in the GSH/GSSG ratio. In addition, the cellular

redox equilibrium is shifted toward more protein-bound glutathione, with significant increases in protein-bound/total GSH and protein-bound/free GSH ratios. Furthermore, we used monoclonal anti-GSH antibody to investigate protein glutathionylation in fibroblasts, and we found that proteins are glutathionylated in FRDA, with a 5-fold increase in FRDA patients.

Protein glutathionylation occurs also in normal fibroblasts, but to a lower extent. The fact that some proteins are constitutively glutathionylated under basal conditions has already been observed by Fratelli *et al.* (37) in T lymphocytes and may indicate a regulatory role for glutathionylation in several protein functions. In normal liver, for instance, 20–30 nmol of glutathione/g of liver are present as disulfides mixed with proteins (41).

Many proteins can undergo glutathionylation under oxida-

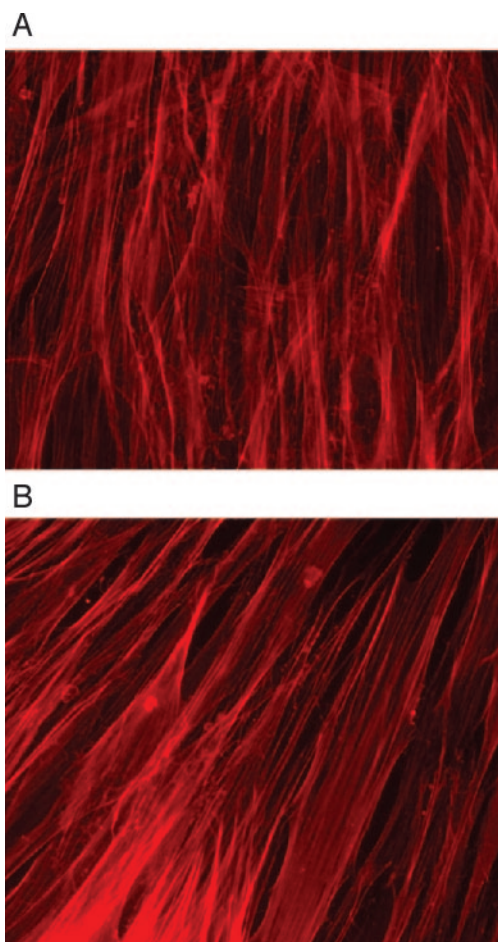


FIG. 7. Fluorescent images of control fibroblasts after *in vivo* FeSO₄ treatment. Control cells (A) were treated *in vivo* with 100 μ M FeSO₄ for 30 days at 37 °C (B), and actin was visualized by rhodamine phalloidin staining.

tive stress (36, 42, 43). Some proteins sustain different but important functions, such as nucleophosmin (involved in the assembly of ribosomal proteins), cyclophilin (a chaperonin involved in the proteasomal degradation of proteins), and the heat shock proteins HSP60 and HSP70. Glyceraldehyde-3-phosphate dehydrogenase is the major *S*-glutathionylated protein in endothelial cells exposed to hydrogen peroxide and in monocytes during the endogenous oxidative burst (23, 44). Creatine kinase and glycogen phosphorylase *b* are also targets for *S*-glutathionylation in myocytes and cardiac tissue during cyclic oxidative stress. Carbonic anhydrase III, glutathione *S*-transferase, superoxide dismutase, hemoglobin, and bovine eye lens crystalline become thiolated in cellular models of oxidative stress. Additional proteins, including fatty-acid synthase, 3-hydroxy-3-methylglutaryl-CoA reductase, aldose reductase, human immunodeficiency virus-1 protease, and small HSP25, have been reported as potential targets *in vitro* for redox-dependent *S*-glutathionylation (36). Even *c*-Jun DNA binding appears to be redox-regulated by glutathionylation (27, 28), and dopamine biosynthesis is also inhibited by *S*-glutathionylation during oxidative stress (45). In Parkinson's disease, monoamine oxidase-derived H₂O₂ was shown to inhibit mitochondrial respiration by glutathionylation of respiratory chain enzymes (46). Finally, direct glutathionylation of proteins by superoxide anion has been demonstrated in a study showing that *S*-glutathionylation of protein-tyrosine phosphatases modulates the phosphorylation state of cells and preserves protein function (47).

Some of the proteins found to be glutathionylated belong to the class of cytoskeletal proteins, which are particularly abundant in cells. The supramolecular organization of these proteins depends on the presence of exposed sulfhydryl residues; the modification of these groups by glutathionylation could be relevant to their function, by either protecting them against irreversible oxidation or inhibiting polymerization (48–50).

In this study, we have demonstrated that the glutathionylation of actin caused an impairment of microfilaments dynamic in FRDA fibroblasts, as showed using the filamentous actin indicator rhodamine phalloidin. The fluorescent images revealed a marked and diffuse reduced signal of F-actin, probably due to disassembly of actin filaments. The same hematoxylin/eosin-stained cells showed clear abnormalities in size and shape. Also, the viability of FRDA fibroblasts was $18.7 \pm 4.3\%$ lower than that of control cells as measured by flow cytometric analysis using 6-carboxyfluorescein.

Actin is one of the major cytoskeletal proteins, playing an important role in mediating the infrastructure and dynamics of the cytoplasmic matrix. Its polymerization is a dynamic process implicated in growth factor-mediated cytoskeletal changes. Wang *et al.* (30) directly linked the epidermal growth factor-mediated signaling pathway to *in vivo* de-glutathionylation of actin with an increase in F-actin, thus highlighting protein glutathionylation as a physiologically relevant regulatory mechanism in actin polymerization. Monitored by light scattering, the steady-state rate for non-glutathionylated actin polymerization was at least 5.6-fold faster than that for glutathionylated actin polymerization obtained in the presence of GSSG (30). Recently, Dalle-Donne *et al.* (50) demonstrated *in vitro* that glutathionylated actin has a decreased capacity to polymerize compared with native actin, with filament elongation being inhibited. An impaired microfilament organization by glutathione binding has been reported in rabbit muscle, where the addition of glutathione at Cys³⁷⁴ of actin resulted in filaments with a diminished mechanical stability (51, 52).

The glutathionylation of actin has been observed in several cells under varying conditions of oxidative stress, *e.g.* gastric mucosal cells treated with H₂O₂ or diamide and phorbol myristate acetate-stimulated murine macrophages and human neutrophils (48, 53). H₂O₂ treatment is also responsible for actin glutathionylation in human epidermal carcinoma A431 cells, where it regulates actin polymerization (30).

A role of oxidized actin has been reported in some neurodegenerative diseases, such as in a mouse model of amyotrophic lateral sclerosis, where axonal degeneration appears to be due to defective transport of components required for axonal maintenance (54). Actin oxidation was significantly higher even in brain extracts of patients with Alzheimer's disease, suggesting that oxidative stress-induced injury may lead to the degeneration of neurons in the Alzheimer's disease brain (55).

Glutathionylation is a redox-dependent reversible mechanism (30, 50). Indeed, when we incubated fibroblasts with pro-oxidants *in vitro*, we found a 4-fold increase in glutathionylation in the presence of GSSG and a 2.5-fold increase with H₂O₂. Glutathionylation was also reversed *in vitro* by excess GSH or dithiothreitol (data not shown). To address the *in vivo* reversibility of actin glutathionylation in FRDA, we treated fibroblasts with GSH for 1 month and evaluated the extent of glutathionylation and cell morphology. Interestingly, we found a 60% decrease in protein glutathionylation in treated fibroblasts upon analysis by Western blotting and a complete rescue of size and cell shape. Even cell viability resulted in a significant enhancement of the fluorescent signal in GSH-treated FRDA cells, becoming comparable to that in controls.

GSH transport across cell membrane is not yet well defined,

although some studies have provided insight especially on GSH release, which seems to involve the family of multidrug resistance-associated proteins (32). Evidence for direct uptake of glutathione has been shown only in mitochondria, where the dicarboxylate and 2-oxoglutarate carriers were identified in the inner membrane (56, 57). Therefore, to elucidate how medium GSH is available to the cells, we treated FRDA fibroblasts *in vivo* with acivicin, an inhibitor of γ -glutamyltranspeptidase, and we found that acivicin blocked the protection obtained by GSH treatment, whereas EE-GSH continued to act (data not shown). Thus, GSH does not seem to be directly taken up by the cells, whereas the action of EE-GSH, which is membrane-permeable, is not affected by the inhibitor. Therefore, the availability of medium GSH to the cells seems to be mediated by γ -glutamyltranspeptidase, although further studies will be necessary to better elucidate the mechanism underlying the *in vivo* effect of glutathione treatments, also in light of the unexpected lesser effectiveness of EE-GSH with respect to GSH, on the protein-bound GSH levels.

Iron-mediated oxidative damage has been proposed to underlie the pathogenesis of FRDA. Our findings directly link iron overload and actin glutathionylation, as demonstrated by *in vivo* treatments of control fibroblasts with FeSO_4 . HPLC analysis showed a significant increase in the protein-bound/free GSH ratio, and Western blot analysis indicated a relevant rise in glutathionylation in FeSO_4 -treated fibroblasts compared with untreated cells. Taken together, our data suggest a role for iron-mediated oxidative stress in the abnormally enhanced glutathionylation in FRDA. However, we did not observe any significant morphological changes resembling those of FRDA fibroblasts after FeSO_4 treatment of control cells. Thus, the morphological changes observed in FRDA cells probably reflect an abnormal cellular response to chronic iron overload, which in controls is balanced by the presence of frataxin; but it is, however, enough to be transduced into protein glutathionylation.

In conclusion, we speculate that intracellular iron imbalance due to frataxin deficiency leads to oxidative stress in FRDA, inducing actin glutathionylation and impairment of cytoskeletal functions. This underlying pathogenic mechanism may contribute to the progression of neurodegeneration in the disease.

REFERENCES

- Puccio, H., and Koenig, M. (2000) *Hum. Mol. Genet.* **9**, 887–892
- Patel, P. I., and Isaya, G. (2001) *Am. J. Hum. Genet.* **69**, 15–24
- Pandolfo, M. (1999) *Arch. Neurol.* **56**, 1201–1208
- Knight, S. A. B., Kim, R., Pain, D., and Dancis, A. (1999) *Am. J. Hum. Genet.* **64**, 365–371
- Radisky, D. C., Babcock, M. C., and Kaplan, J. (1999) *J. Biol. Chem.* **274**, 4497–4499
- Edmond, M., Simon, D., Cossee, M., Crique-Filipe, P., Tiziano, F., Melki, J., Hindelang, C., Matyas, R., Rustin, P., and Koenig, M. (2001) *Nat. Genet.* **27**, 181–186
- Delatycki, M. B., Camakaris, J., Brooks, H., Evans-Whipp, T., Thorburn, D. R., Williamson, R., and Forrest, S. M. (1999) *Ann. Neurol.* **45**, 673–675
- Wong, A., Yang, J., Cavadini, P., Gellera, C., Lonnerdal, B., Taroni, F., and Cortopassi, G. (1999) *Hum. Mol. Genet.* **8**, 425–430
- Bradley, J. L., Blake, J. C., Chamberlain, S., Thomas, P. K., Cooper, J. M., and Schapira, A. H. V. (2000) *Hum. Mol. Genet.* **9**, 275–282
- Vorgerd, M., Schols, L., Hardt, C., Ristow, M., Epplen, J. T., and Zange, J. (2000) *Neuromuscular Disorders* **10**, 430–435
- Edmond, M., Lepage, G., Vanasse, M., and Pandolfo, M. (2000) *Neurology* **55**, 1752–1753
- Schulz, J. B., Dehmer, T., Schols, L., Mende, H., Hardt, C., Vorgerd, M., Burk, K., Matson, W., Dichgans, J., Beal, M. F., and Bogdanov, M. B. (2000) *Neurology* **55**, 1719–1721
- Lodi, R., Hart, P. E., Rajagopalan, B., Taylor, D. J., Phil, D., Crilley, J. G., Bradley, J. L., Blamire, A. M., Manners, D., Styles, P., Schapira, A. H., and Cooper, J. M. (2001) *Ann. Neurol.* **49**, 590–596
- Lerman-Sagie, T., Rustin, P., Lev, D., Yanov, M., Leshinsky-Silver, E., Sagie, A., Ben-Gal, T., and Munnich, A. (2001) *J. Inher. Metab. Dis.* **24**, 28–34
- Housse, A. O., Aggoun, Y., Bonnet, D., Sidi, D., Munnich, A., Rotig, A., and Rustin, P. (2002) *Heart (Lond.)* **87**, 346–349
- Tozzi, G., Nuccetelli, M., Lo Bello, M., Bernardini, S., Bellincampi, L., Ballerini, S., Gaeta, L. M., Casali, C., Pastore, A., Federici, G., Bertini, E., and Piemonte, F. (2002) *Arch. Dis. Child.* **86**, 376–380
- Piemonte, F., Pastore, A., Tozzi, G., Tagliacozzi, D., Santorelli, F. M., Carozzo, R., Casali, C., Damiano, M., Federici, G., and Bertini, E. (2001) *Eur. J. Clin. Invest.* **31**, 1007–1011
- Gilbert, H. F. (1995) *Methods Enzymol.* **251**, 8–28
- Gilbert, H. F. (1982) *J. Biol. Chem.* **257**, 12086–12091
- Ernest, M. J., and Kim, K. H. (1974) *J. Biol. Chem.* **249**, 5011–5018
- Nakashima, K., Horecker, B. L., and Pontremoli, S. (1970) *Arch. Biochem. Biophys.* **141**, 579–587
- Cappel, R. E., and Gilbert, H. F. (1989) *J. Biol. Chem.* **264**, 9180–9187
- Ravichandran, V., Seres, T., Moriguchi, T., Thomas, J. A., and Johnston, R. B. (1994) *J. Biol. Chem.* **269**, 25010–25015
- Ward, N. E., Pierce, D. S., Chung, S. E., Gravitt, K. R., and O'Brian, C. A. (1998) *J. Biol. Chem.* **273**, 12558–12566
- Brandwein, H. J., Lewicki, J. A., and Murad, F. (1981) *J. Biol. Chem.* **256**, 2958–2962
- Silva, C. M., and Cidiowski, J. A. (1989) *J. Biol. Chem.* **264**, 6638–6647
- Klatt, P., Molina, E. S., Lacoba, M. C., Padilla, C. A., Mrtinez-Glaisteo, E., Barcena, J. A., and Lamas, S. (1999) *FASEB J.* **13**, 1481–1490
- Klatt, P., Molina, E. P., and Lamas, S. (1999) *J. Biol. Chem.* **274**, 15857–15864
- Jahnegen-Hodge, J., Obin, M. S., Gong, X., Shang, F., Novell, T. R., Gong, J., Abasi, H., Blumberg, J., and Taylor, A. (1997) *J. Biol. Chem.* **272**, 28218–28226
- Wang, J., Boja, E. S., Tan, W., Tekle, E., Fales, H. M., English, S., Mieyal, J. J., and Cock, B. (2001) *J. Biol. Chem.* **276**, 47763–47766
- Reddy, S., Jones, A. D., Cross, C. E., Wong, P. S. Y., and Van der Vliet, A. (2000) *Biochem. J.* **347**, 821–827
- Hayes, J. D., and McLellan, L. I. (1999) *Free Radic. Res.* **31**, 273–300
- Fernandez-Checa, J. C., Kaplowitz, N., Garcia-Ruiz, C., Colell, A., Miranda, M., Mari, M., Ardite, E., and Morales, A. (1997) *Am. J. Physiol.* **273**, G7–G17
- Schulz, J. B., Lindenau, J., Seyfried, J., and Dichgans, J. (2000) *Eur. J. Biochem.* **267**, 4904–4911
- Sofic, E., Lange, K. W., Jellinger, K., and Riederer, P. (1992) *Neurosci. Lett.* **142**, 128–130
- Klatt, P., and Lamas, S. (2000) *Eur. J. Biochem.* **267**, 4928–4944
- Fratelli, M., Demol, H., Puype, M., Casagrande, S., Eberini, I., Salmons, M., Bonetto, V., Mengozzi, M., Duffieux, F., Milet, E., Bachi, A., Vandekerckhove, J., Gianazza, E., and Ghezzi, P. (2002) *Proc. Natl. Acad. Sci. U. S. A.* **99**, 3505–3510
- Pastore, A., Piemonte, F., Locatelli, M., Lo Russo, A., Gaeta, L. M., Tozzi, G., and Federici, G. (2001) *Clin. Chem.* **47**, 1467–1469
- Lamarche, J. B., Shapcott, D., Cote, M., and Lemieux, B. (1993) in *Handbook of Cerebellar Diseases* (Lechtenberg, R., ed) pp. 453–456, Marcel Dekker, Inc., New York
- Walvogel, D., van Gelderen, P., and Hallett, M. (1999) *Ann. Neurol.* **46**, 123–125
- Brigelius, R., Muckel, C., Akerboom, T. P., and Sies, H. (1983) *Biochem. Pharmacol.* **32**, 2529–2534
- Cotgreave, I. A., and Gerdes, R. G. (1998) *Biochem. Biophys. Res. Commun.* **242**, 1–9
- Eaton, P., Byers, H. L., Leeds, N., Ward, M. A., and Shattock, M. J. (2002) *J. Biol. Chem.* **277**, 9806–9811
- Schuppe-Koisenin, I., Moldeus, P., Bergmann, T., and Coatgreave, I. A. (1994) *Eur. J. Biochem.* **221**, 1033–1037
- Borges, C. R., Geddes, T., Watson, J. T., and Kuhn, D. M. (2002) *J. Biol. Chem.* **277**, 48295–48302
- Cohen, G., Farooqui, R., and Kesler, N. (1997) *Proc. Natl. Acad. Sci. U. S. A.* **94**, 4890–4894
- Barrett, W. C., DeGnore, J. P., Keng, Y. F., Zhang, Z. Y., Yim, M. B., and Chock, P. B. (1999) *J. Biol. Chem.* **274**, 34543–34546
- Rokutan, K., Johnson, R. B., and Kaway, K. (1994) *Am. J. Physiol.* **266**, G247–G254
- Dalle-Donne, I., Milazani, A., Giustarini, D., Di Simplicio, P., Colombo, R., and Rossi, R. (2000) *J. Muscle Res. Cell Motil.* **21**, 171–181
- Dalle-Donne, I., Giustarini, D., Rossi, R., Colombo, R., and Milzani, A. (2003) *Free Radic. Biol. Med.* **34**, 23–32
- Chai, Y. C., Ashraf, S. S., Rokutan, K., Johnston, R. B., and Thomas, J. A. (1994) *Arch. Biochem. Biophys.* **310**, 273–281
- Tsapara, A., Kardassis, D., Moustakas, A., Gravanis, A., and Stournaras, C. (1999) *FEBS Lett.* **455**, 117–122
- Stournaras, C., Drewes, G., Blackholm, H., Merkle, I., and Faulstich, H. (1990) *Biochim. Biophys. Acta* **1037**, 86–91
- Collard, J. F., Cote, F., and Julien, J. P. (1995) *Nature* **375**, 12–13
- Aksenoz, M. Y., Aksenova, M. V., Butterfield, D. A., Geddes, J. W., and Markesbery, W. R. (2001) *Neuroscience* **103**, 373–383
- Chen, Z., and Lash, L. H. (1998) *J. Pharmacol. Exp. Ther.* **285**, 608–618
- Pastore, A., Federici, G., Bertini, E., and Piemonte, F. (2003) *Clin. Chim. Acta* **333**, 19–39

Actin Glutathionylation Increases in Fibroblasts of Patients with Friedreich's Ataxia: A POTENTIAL ROLE IN THE PATHOGENESIS OF THE DISEASE

Anna Pastore, Giulia Tozzi, Laura Maria Gaeta, Enrico Bertini, Valentina Serafini, Silvia Di Cesare, Valentina Bonetto, Filippo Casoni, Rosalba Carrozzo, Giorgio Federici and Fiorella Piemonte

J. Biol. Chem. 2003, 278:42588-42595.

doi: 10.1074/jbc.M301872200 originally published online August 11, 2003

Access the most updated version of this article at doi: [10.1074/jbc.M301872200](https://doi.org/10.1074/jbc.M301872200)

Alerts:

- [When this article is cited](#)
- [When a correction for this article is posted](#)

[Click here](#) to choose from all of JBC's e-mail alerts

This article cites 53 references, 22 of which can be accessed free at <http://www.jbc.org/content/278/43/42588.full.html#ref-list-1>